High-Temperature Superconducting Magnets for NMR and MRI: R&D Activities at the MIT Francis Bitter Magnet Laboratory

High-Temperature Superconducting Magnets for NMR and MRI: R&D Activities at the MIT Francis Bitter Magnet Laboratory

Yukikazu Iwasa, Juan Bascuñán, Seungyong Hahn, Masaru Tomita, and Weijun Yao

***Abstract*—This paper describes the NMR/MRI magnets that are currently being developed at the MIT Francis Bitter Magnet Laboratory: 1) a 1.3 GHz NMR magnet; 2) a compact NMR magnet assembled from YBCO annuli; and 3) a persistent-mode, fully-protected MgB_2 0.5-T/800-mm whole-body MRI magnet.**

***Index Terms*—Compact NMR annulus magnet, LTS/HTS NMR magnet, MgB_2 MRI magnet.**

I. Introduction

A TREMENDOUS progress achieved in the past decade and is continuing today has transformed selected HTS materials into "magnet-grade" conductors, i.e., meet rigorous magnet specifications and are *readily* available from commercial wire manufacturers [1]. We are now at the threshold of a new era in which HTS will play a key role in a number of applications—here $MgB_2 (T_c = 39\ \mathrm{K})$ is classified as an HTS. The HTS offers opportunities and challenges to a number of applications for superconductivity. In this paper we briefly describe three NMR/MRI magnets programs currently being developed at FBML that would be impossible without HTS: 1) a 1.3 GHz NMR magnet; 2) a compact NMR magnet assembled from YBCO annuli; and 3) a persistent-mode, fully-protected MgB_2 0.5-T/800-mm whole-body MRI magnet.

II. 1.3-GHz LTS/HTS NMR Magnet

In 2000 the National Institutes of Health awarded the FBML Phase 1 program of a 3-phase 1-GHz NMR magnet comprised of an LTS background field NMR magnet and an HTS insert. Although the goal of Phase 1 was modest (350-MHz: 300 MHz LTS; 50 MHz HTS [2], this 3-phase program was first to formally proceed towards a goal to complete a 1-GHz NMR magnet by a combination of LTS and HTS magnets. In 2007, after completion of Phase 2 (700 MHz: 600 MHz LTS; 100 MHz HTS [3], [4]), the target frequency was upgraded to 1.3 GHz.

TABLE I
High-Field LTS NMR Magnets

Frequency [MHz]	900	900	700	500
Center field [T]	21.11	21.11	16.44	11.74
Operating temperature [K]	1.8	4.2	4.2	4.2
Cold bore [mm]	135	135	236	236
Operating current, I_{op} [A]	248.7	180.6	251.0	250.0
Magnetic energy @I_{op} [MJ]	42.5	103	20.9	4.7

The total cost of a >1-GHz LTS/HTS NMR magnet is driven chiefly by the cost of a background LTS magnet. Generally, the lower the field, the lower the cost of a high-field LTS NMR magnet even though a lower field obviously requires a wider *cold* bore, because the companion HTS insert must be larger to make up for the LTS magnet.

Table I lists key magnet and operating parameters of four high-field/wide-bore LTS NMR magnets: 900 MHz (at 1.8 K and 4.2 K), 700 MHz and 500 MHz (both at 4.2 K), prepared by Yoshikawa [5]. Fig. 1 presents in-scale cross sectional profiles of 4 magnets listed in Table I: from top to bottom, left to right are 900 MHz/135 mm cold bore LTS magnet operating at 1.8 K (L900/135/1.8); L900/135/4.2; L700/236/4.2, and L500/236/4.2. The stored magnetic energy for each magnet is given in parentheses.

Note that L900 has two versions, one operating at 1.8 K and the other at 4.2 K. At 1.8 K the performance of Nb_3Sn coils is superior to that at 4.2 K, particularly at fields above ~19 T (~800 MHz). At 750 MHz and below the incremental gain in the performance of Nb_3Sn coils is negated by increased system complexity and extra cost associated with operation at 1.8 K. Also note that the gain in HTS performance achieved at sub-4.2 K operation is negligible but its slight resistance, due chiefly to splices and index dissipation, makes 1.8-K operation substantially more expensive, cryogenically, than 4.2-K operation.

L700/H600 Choice: For a 1-GHz LTS/HTS NMR magnet, 900 MHz is the "traditional" choice for the LTS magnet (L900), the choice of the groups currently working on or planning 1 GHz and above LTS/HTS NMR magnets. This was our choice in 1999 at the outset of our 3-phase program with the ultimate goal of 1 GHz at the conclusion of Phase 3. However, because the cost of an LTS magnet, as may be inferred from the magnetic energies of the LTS magnets shown in Table I and listed in

Manuscript received October 20, 2009. First published March 04, 2010; current version published May 28, 2010. This work was supported by the National Center for Research Resources (NCRR), the National Institute of Biomedical Imaging and Bioengineering (NIBIB), and the National Institute of General Medical Sciences (NIGMS).

Y. Iwasa, J. Bascuñán, S. Hahn, and W. Yao are with the MIT Francis Bitter Magnet Laboratory (FBML), Cambridge, MA 02139 USA (e-mail: iwasa@jokaku.mit.edu)

M. Tomita was with the MIT Francis Bitter Magnet Laboratory (FBML), Cambridge, MA 02139 USA. He is now with the Railway Technical Research Institute, Tokyo, Japan, and is also a collaborator with the Compact NMR Annulus Magnet project.

Color versions of one or more of the figures in this paper are available online at http://ieeexplore.ieee.org.

Digital Object Identifier 10.1109/TASC.2010.2040073

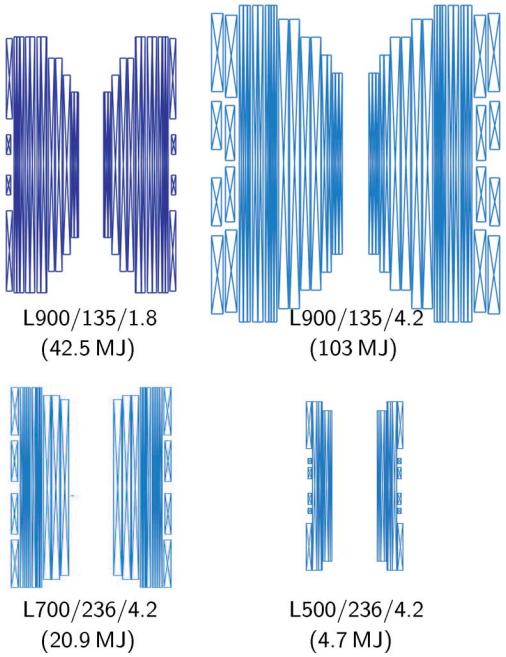

Fig. 1. In-scale cross sectional profiles of 4 LTS ($\mathrm{NbTi}/\mathrm{Nb_3Sn}$) magnets listed in Table I. The 900-MHz, 700-MHz, and 500-MHz LTS magnets in Table I are designated, respectively, as L900, L700, and L500. The stored magnetic energy for each magnet is given in parentheses. [5]

Fig. 1, increases sharply more with field than bore size, we now believe that to reduce the overall cost of a $>$ 1-GHz LTS/HTS NMR magnet, L900 may not be an optimal choice.

Our choice of a L700/H600 division for a 1.3 GHz magnet is to balance the decreasing cost of an LTS magnet on one hand and increasing technical challenges of an HTS insert on the other. For example, an L700 with a cold bore of 236 mm operating at 4.2 K has a magnetic energy nearly 1/5th that of an L900 with a cold bore of only 135 mm operating at 4.2 K. Note also that a cold bore of 135 mm is just sufficient to accommodate an HTS insert generating no greater than 200 MHz, i.e., it is not possible to achieve a field of 1.3 GHz with a 900-MHz LTS magnet, operated at 1.8 K or 4.2 K, having a cold bore of 135 mm. A 900-MHz LTS magnet having a cold bore of 236 mm will surely have a magnetic energy in excess of 100 MJ (1.8 K) and that approaching 300 MJ (4.2 K) or over 10 times that of a 700 MHz/236 mm LTS magnet.

H600: The 600-MHz HTS insert consists of two nested stacks of double-pancake coils, each wound with HTS tape, YBCO, Bi2223, or even a combination of both. One serious problem for a high-resolution NMR magnet comprising a tape-wound magnet is a large screening-current field (SCF) or a remanent field that will degrade spatial field homogeneity [6]–[8]. (Note that in AC devices, SCF is the source of hysteresis losses.) Our H600 will not escape this problem. We plan to install a set of superconducting shimming coils in an L700, specifically targeted to minimize SCF-induced harmonic errors.

Our current targeted years for completion of 1.1-GHz and 1.3-GHz systems are, respectively, 2012 and 2016–2017.

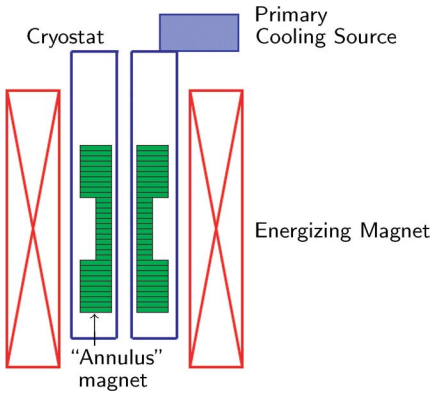

Fig. 2. Schematic drawing of a compact NMR "annulus" magnet, *at the manufacturing site*. The system—here only its essential components are included—consists of: 1) annulus magnet, 2) cryostat, 3) an energizing electromagnet, and 4) a primary cooling source.

III. Compact NMR "Annulus" Magnet

In July 2009 we began a 2-phase program to develop *compact* NMR magnets assembled from YBCO annuli [9]. It is only with HTS that this design option is feasible. A stack may be of thick (bulk) annuli or thin (plate or coated tape) annuli [1]. The goals of this 2-phase program are to complete: 1) in Phase 1 a prototype compact annulus magnet of an NMR-quality field homogeneity operating in the frequency range 100–200 MHz with a room-temperature (RT) bore of 10 mm; and 2) in Phase 2 a compact NMR annulus magnet in the frequency range 300–500 MHz with an RT bore of 36 mm, which will be suitable for high-resolution microspectroscopy or "microcoil" NMR [10].

We believe that a *compact*, *simple-to-manufacture*, and *easy-to-operate* NMR magnet will have a widespread use in pharmaceutical and food industries for discovery and development of drugs and food sources and even in medical centers as a new tool for efficient delivery of medical care, e.g., evaluation of the effects of a drug on the patient.

For a "high-field" compact magnet, bulk annuli have an advantage over plate annuli because the cross sectional area of bulk disks is almost entirely occupied by superconducting YBCO, while the opposite is the case with YBCO plates. The engineering critical current density, J_e, is thus at least one order of magnitude greater for bulk than for plate [1]. The Phase 1 compact NMR annulus magnet is an assembly of bulk annuli prepared from high-performance YBCO bulk disks [11]. Athough lacking in J_e but because each plate is thin ($\sim$0.1 mm vs. $\sim$10 mm for bulk), plate annuli could be useful to improve the spatial field homogeneity of the Phase 1 annulus magnet. The Phase 1 activities, therefore, include study of magnetic behavior, both analytical and experimental, of plate annuli, individuals and groups in a stack [12].

Fig. 2 shows a schematic drawing of an annulus magnet where the magnet is energized—in the marketplace at the manufacturer site. The system consists of an annulus magnet—note that the o.d. of the annuli in the middle section is reduced to create a "notch" to symbolically indicate that the annuli assembly is designed to generate a spatially homogeneous field about the center, a cryostat for the annulus magnet, an

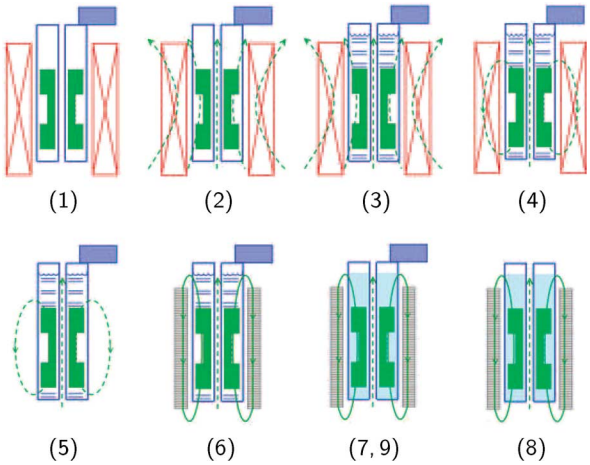

Fig. 3. Schematic drawings of a compact NMR annulus magnet system over 9 steps. *Step 1*: the initial stage when the annulus magnet is still at room temperature; *Step 8*: the penultimate stage when the system, sans its primary cooling source, is ready for shipment from the manufacture site to the user site. With a cooling source installed to the system at the user site, the system is ready for use, a schematic drawing of which is identical to *Step 7*.

energizing electromagnet to field-cool the annulus magnet, and a primary cooling source to keep the cold body (the magnet and a volume solid nitrogen) at an operating temperature of, e.g., 20 K. The figure omits annulus steel sheets required and added before shipment of the system to the user site to reduce the fringing field, and mechanical, electrical, other cryogenic components. The role of solid nitrogen is described later.

Because the annulus magnet is designed to be energized at its manufacturing site, where a large energizing electromagnet is stationed, and transported to the user site, the cryogenic system, with a fully-energized magnet, must possess sufficient heat capacity to keep the magnet, during the site-to-site shipment within an acceptable range of temperatures, cooled by solid cryogen, here, nitrogen.

Procedure: From Manufacturing Site to User Site: The entire procedure for energizing an annulus magnet at the manufacturer site and delivering the energized annulus magnet ready at the user site consists of the following nine steps, illustrated in Fig. 3.

Step 1) (Fig. 3-1) Place the annulus magnet, still at room temperature, into a cryostat, which is already in the bore of an energizing electromagnet.

Step 2) (Fig. 3-2) Energize the electromagnet to a field strength so that when the annulus magnet is "field-cooled" (*Step 4*), its central field is nearly equal to its nominal operating field—see below why "nearly".

Step 3) (Fig. 3-3) Fill the cryostat with liquid nitrogen (77.3 K), cooling the annulus magnet well below its superconducting critical temperature (93 K). Turn on the primary cooling source (a cryocooler or cryocirculator [1]).

Step 4) (Fig. 3-4) With the annulus magnet cooled down to ~30 K, discharge the energizing electromagnet to zero field, leaving the annulus magnet with a "trapped" field, which at the magnet center is slightly less than the operating field, to be reached later when steel annular sheets are placed outside the cryostat to reduce the fringing field.

Because YBCO is a Type II superconductor, which is dissipative when exposed to a time-varying magnetic field, the field discharge rate must be sufficiently slow to control the rate of dissipation generated within each annulus. To facilitate conduction of this internal heat dissipation to the solid nitrogen that surrounds the magnet, a thin, high-thermal-conductive, high-strength normal metal, e.g., CuNi alloy, spacer will be placed between annuli. The metal spacers also reinforce the magnet assembly and with its thickness as a variable, it may also be used to improve the spatial field homogeneity. Note that the magnetic field is now generated entirely by the annulus magnet.

The energized annulus magnet is now ready to be prepared for shipment to the user site—*Steps 5–8*.

Step 5) (Fig. 3-5) Remove the energized annulus magnet from the electromagnet.

Step 6) (Fig. 3-6) Place steel annuli outside the cryostat along its axial length. The radial build of the steel annuli are chosen to make the fringe field at the annulus magnet midplane and 1-m radius from the magnet center <5 gauss.

The magnetized steel outside the cryostat enhances the center field. Thus the initial charging field, generated by the energizing electromagnet, must be set to a level that results in the desired annulus magnet center field *after* it is field-cooled *and* shielded with steel annuli. Also, note that the spatial field homogeneity will also be modified after placement of the shielding assembly. It means that a field analysis to determine not only the energizing field but also precise dimensions of each annulus must include the presence of the shielding assembly.

Step 7) (Fig. 3-7) For packing the energized and shielded annulus magnet for shipment, further cool the cold body to ~15 K.

Step 8) (Fig. 3-8) Disengage the primary cooling source from the system. Pack and ship the system to the user site. With no cooling the cold body—the annulus magnet and the solid nitrogen—warms up. The cryostat design and the amount of solid nitrogen in the cold body must be such that over a ~48-hour period during shipment and when the system is re-connected to another primary cooling source at the user site, the cold body must remain well below ~30 K, the field-cooling temperature. With high heat capacity substance such as solid nitrogen in the cold body, this requirement of a small temperature rise (less than ~10 K) over a period of ~48 h in the absence of a cooling source is achievable.

IV. MgB_2 Whole-Body MRI Magnet

Medical imaging is critical for quality health care for early detection and efficient treatment of disease and injury. Although there are now over 30 000 MRI units in service worldwide, they

TABLE II
AN MgB_2 0.5-T WHOLE-BODY MRI MAGNET

Magnet Segments	MAIN		CORRECTION	
Coil (Pair/Coil)	Coil M1	Coil M2	Coil C1	Coil C2
Winding i.d./o.d. [mm]	860.0 / 877.6		860. / 894.9	
Winding length [mm]	84	71	50	53
*Coil midpoint** [mm]	±94	±279.5	±465	±549.5
Turns/layer	83–84	70–71	49–50	52–53
Layers/Coil	10	10	20	20
Turns/Coil	835	705	990	1050
Wire length/Coil [km]	2.29	1.94	2.76	2.92
Wire length/Segment [km]	8.5		11.4	
Operating Temperature [K]	10 (nominal); 15 (maximum)			
Operating Current, I_{op} [A]	97.8			
λJ_{op}† *@I_{op}* [A/mm^2]	110.5	110.4	111.0	111.1
Peak Field @I_{op} [T]	0.84	0.82	1.27	1.36
Self Inductance/Coil [H]	1.19	0.89	1.87	2.07
Total inductance [H]	25.08			

* Axial location measured from magnet axial center.
† Overall current density.

benefit only ∼10% of the total humanity, chiefly in the *urban* areas of the *developed* nations. Recognizing this glaring disparity in medical treatment opportunities, specifically to those in the developing nations who have no access to medical-imaging health care, the NIBIB launched, in early 2000s, a program to promote development of *low-cost* and *easy-to-operate* MRI magnets.

Under this NIBIB program we began in 2003 to develop a 0.5-T whole-body MRI magnet, wound with MgB_2 wire that can operate without reliance on liquid helium (LHe). Validity of commercially available MgB_2 for a "large-bore" magnet and its operation LHe-free was proven with a "demonstration" magnet [13]. Table II lists key parameters of a new MgB_2 0.5-T/800-mm bore whole-body MRI magnet to be completed in this continuation program.

Our 0.5-T/800-mm whole-body MRI magnet has the following features that are distinct from "conventional" MRI magnets now widely available in the marketplace: 1) MgB_2 vs. NbTi wire; 2) 10-K vs. 4.2-K operation; 3) solid nitrogen vs. LHe. A combination of these features makes 10-K operated MgB_2 magnets, even in the absence of liquid helium, at least an order of magnitude more stable than NbTi counterparts against disturbances that still afflict most NbTi MRI magnets, at least when the NbTi MRI magnets are energized for the first time.

As with the conventional NbTi MRI magnets, our MgB_2 MRI magnet operates in persistent mode and is fully protected. Persistent-mode operation of our magnet is feasible because of a technique to make superconducting MgB_2–MgB_2 multifilamentary wires developed at FBML [14]. Recent data show these joints have self-field critical currents of 245 A (@10 K), 150 A (15 K), 120 A (20 K), 84 A (25 K), 54 A (30 K), and 27 A (35 K) [15].

V. CONCLUSIONS

For high-field and/or >10-K superconducting magnets, HTS is indispensable. This is becoming increasingly clear for NMR and MRI magnets, examples of which are those described here currently on-going at the MIT Francis Bitter Magnet Laboratory. None of these magnets is possible with LTS alone: a 1.3-GHz (30.53 T) NMR; compact NMR annulus (∼20 K); or MgB_2 MRI (10–15 K).

ACKNOWLEDGMENT

The authors thank NCRR, NIBIB, and NIGMS of the National Institutes of Health for support of the magnet projects at FBML. We also thank Dr. John Voccio of American Superconductor Corp. (AMSC) and AMSC for their interest in our annulus magnet project and generous supply of plate annuli prepared from YBCO coated tape.

REFERENCES

[1] Y. Iwasa, *Case Studies in Superconducting Magnets*, 2nd ed. : Springer, 2009.
[2] J. Bascuñán, E. Bobrov, H. Lee, and Y. Iwasa, "A low- and high-superconducting (LTS/HTS) NMR magnet: Design and performance results," *IEEE Trans. Appl. Superconduc.*, vol. 13, p. 1550, 2003.
[3] S. Hahn, J. Bascuñán, H. Lee, E. S. Bobrov, W. Kim, and Y. Iwasa, "Development of a 700 MHz low-/high-temperature superconductor for nuclear magnetic resonance magnet: Test results and spatial homogeneity improvement," *Rev. Sci. Instrum.*, vol. 79, p. 026 105, 2008.
[4] S.-Y. Hahn, J. Bascuñán, H. Lee, E. S. Bobrov, W. Kim, M. Cheol Ahn, and Y. Iwasa, "Operation and performance analyses of 350 and 700 MHz low-/high-temperature superconductor nuclear magnetic resonance magnets: A march toward operating frequencies above 1 GHz," *J. Appl. Phys.*, vol. 105, p. 024 501, 2009.
[5] M. Yoshikawa, 2006, personnal communication.
[6] C. Gu, T. Qu, and Z. Han, "Measurement and calculation of residual magnetic field in a Bi2223/Ag Magnet," *IEEE Trans. Appl. Superconduct.*, vol. 17, p. 2394, 2007.
[7] N. Amemiya and K. Akachi, "Magnetic field generated by shielding current in high T_c superconducting coils for NMR magnets," *Supercond. Sci. Technolo.*, vol. 21, p. 095 001, 2008.
[8] M. Cheol Ahn, T. Yagai, S. Hahn, R. Ando, J. Bascuñán, and Y. Iwasa, "Spatial and temporal variations of a screening current induced magnetic field in a double-pancake HTS insert of an LTS/HTS NMR magnet," *IEEE Tran. Appl. Superconduc.*, vol. 19, p. 2269, 2009.
[9] Y. Iwasa, S.-Y. Hahn, M. Tomita, H. Lee, and J. Bascuñán, "A 'persistent-mode' magnet comprised of YBCO annuli," *IEEE Trans. Appl. Superconduc.*, vol. 15, p. 2352, 2005.
[10] D. L. Olson, T. L. Peck, A. G. Webb, R. L. Magin, and J. V. Sweedler, "High resolution microcoil ^{1}H-NMR for mass-limited, nanoliter-volume samples," *Science*, vol. 270, p. 1967, 1995.
[11] M. Tomita and M. Murakami, "High-temperature superconductor bulk magnets that can trap magnetic fields of over 17 tesla at 29 K," *Nature*, vol. 421, p. 517, 2003.
[12] S. Hahn, S. Beom Kim, M. Cheol Ahn, J. Voccio, J. Bascuñán, and Y. Iwasa, "Trapped field characteristics of stacked YBCO thin plates for compact NMR magnets: Spatial field distribution and temporal stability," *IEEE Trans. Appl. Superconduc.*, vol. 20, 2010, in this issue.
[13] W. Yao, J. Bascuñán, W.-S. Kim, S. Hahn, H. Lee, and Y. Iwasa, "A solid nitrogen cooled MgB_2 'demonstration' coil for MRI applications," *IEEE Trans. Appl. Superconduc.*, vol. 18, p. 912, 2008.
[14] W. Yao, J. Bascuñán, S. Hahn, and Y. Iwasa, "A superconducting joint technique for MgB_2 round wires," *IEEE Trans. Appl. Superconduc.*, vol. 19, 2009.
[15] W. Yao, J. Bascuñán, S. Hahn, and Y. Iwasa, " MgB_2 coil for MRI applications," *IEEE Trans. Appl. Superconduc.*, vol. 20, 2010, in this issue.